JOURNAL OF AGRICULTURAL AND FOOD CHEMISTRY
ARTICLE

J. Agric. Food Chem. 2010, 58, 8833–8841 8833
DOI:10.1021/jf101571z

Pterostilbene Inhibits Colorectal Aberrant Crypt Foci (ACF) and Colon Carcinogenesis via Suppression of Multiple Signal Transduction Pathways in Azoxymethane-Treated Mice

Yi-Siou Chiou,[†] Mei-Ling Tsai,[†] Ying-Jan Wang,[§] An-Chin Cheng,[#] Wei-Ming Lai,[⊥] Vladimir Badmaev,[⊗] Chi-Tang Ho,*[,△] and Min-Hsiung Pan*[,†]

[†]Department of Seafood Science, National Kaohsiung Marine University, Kaohsiung 811, Taiwan, [§]Department of Environmental and Occupational Health, National Cheng Kung University Medical College, Tainan 704, Taiwan, [#]Department of Nutrition and Health Sciences, Chang Jung Christian University, Tainan 71101, Taiwan, [⊥]Departhment of Pathology and Laboratory Medicine, Kaohsiung Veterans General Hospital, Kaohsiung 81362, Taiwan, [⊗]Sabinsa Corporation, 70 Ethel Road West Unit 6, Piscataway, New Jersey 08854, and [△]Department of Food Science, Rutgers University, New Brunswick, New Jersey 08901-8520

Pterostilbene (PS), a natural dimethylated analogue of resveratrol, is known to have diverse pharmacologic activities including anticancer, anti-inflammation, antioxidant, apoptosis, antiproliferation, and analgesic potential. This paper reports the inhibitory effect of dietary administration of pterostilbene against the formation of azoxymethane (AOM)-induced colonic aberrant crypt foci (ACF) preneoplastic lesions and adenomas in male ICR mice and delineates its possible molecular mechanisms. ICR mice were given two AOM injections intraperitoneal and continuously fed a 50 or 250 ppm pterostilbene diet for 6 or 23 weeks. It was found that the dietary administration of pterostilbene effectively reduced AOM-induced formation of ACF and adenomas and inhibited the transcriptional activation of iNOS and COX-2 mRNA and proteins in mouse colon stimulated by AOM. Treatment with pterostilbene resulted in the induction of apoptosis in mouse colon. Moreover, administration of pterostilbene for 23 weeks significantly suppressed AOM-induced GSK3β phosphorylation and Wnt/β-catenin signaling. It was also found that pterostilbene significantly inhibited AOM-induced expression of VEGF, cyclin D1, and MMPs in mouse colon. Furthermore, pterostilbene markedly inhibited AOM-induced activation of Ras, phosphatidylinositol 3 kinase/Akt, and EGFR signaling pathways. All of these results revealed that pterostilbene is an effective antitumor agent as well as its inhibitory effect through the down-regulation of inflammatory iNOS and COX-2 gene expression and up-regulation of apoptosis in mouse colon, suggesting that pterostilbene is a novel functional agent capable of preventing inflammation-associated colon tumorigenesis.

KEYWORDS: Pterostilbene; azoxymethane; aberrant crypt foci; adenomas

INTRODUCTION

Pterostilbene (*trans*-3,5-dimethoxy-4′-hydroxystilbene), a natural dimethylated analogue of resveratrol from blueberries and grape vines, is known to have diverse pharmacologic activities including anticancer, anti-inflammation, antioxidant, antiproliferatory, and analgesic activities (*1*). Our previous studies reported that pterostilbene has the ability to inhibit lipopolysaccharide-induced inflammation in mouse macrophages (*2*), to induce apoptosis and cell cycle arrest (*3*), and to inhibit tumor invasion and metastasis (*4*, *5*). Suh et al. (*6*, *7*) reported that pterostilbene was effective against the formation of azoxymethane-induced colonic aberrant crypt foci (ACF) preneoplastic lesions and colon tumors in male F344 rats.

Colorectal cancer (CRC) is the third most common cause of cancer deaths in men and women in developed countries (*8*). Colon carcinogenesis is a complex multistep process, the adenoma−carcinoma sequence, from small benign precursor lesions to metastatic carcinomas. This progression cascade involves the accumulation of mutation genes as well as the alteration of morphological and cellular events (*9*). Azoxymethane (AOM), a specific carcinogen that induces colorectal tumors at high incidence in rodents, has been widely used in animal models to screen colon cancer preventive agents (*9*).

Previous studies indicate that *β-catenin* and K-*ras* gene mutations frequently occur in AOM-treated murine colon (*11*). Mutations in either *β-catenin* or K-*ras* that lead to the activation of Wnt

*Address correspondence to either author [(M.-H.P.) Department of Seafood Science, National Kaohsiung Marine University, No. 142, Hai-Chuan Rd., Nan-Tzu, Kaohsiung, Taiwan [phone (886)-7-361-7141; fax (886)-7-361-1261; e-mail mhpan@mail.nkmu.edu.tw]; (C.-T.H.) Department of Food Science, Rutgers University, 65 Dudley Rd. New Brunswick, NJ 08901 [fax (732) 932-6776; e-mail ho@aesop.rutgers.edu].

Published on Web 07/20/2010

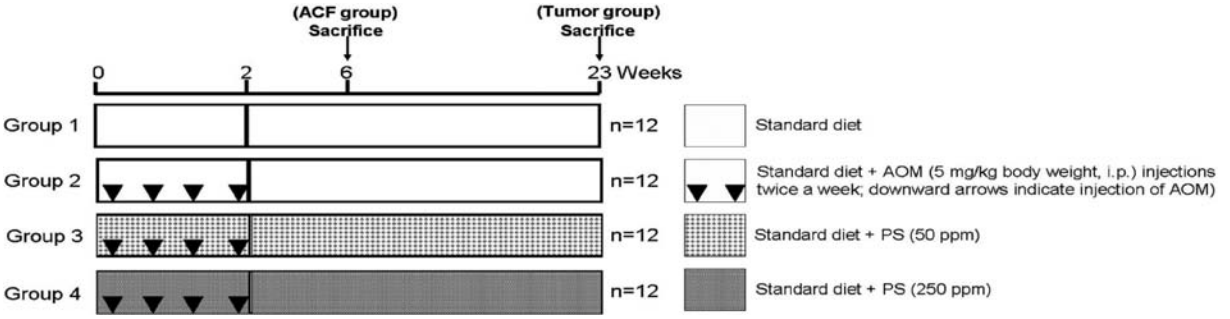

Figure 1. Experimental design of AOM-induced colon carcinogenesis in ICR mice.

signaling pathway are present in the initiation of colorectal carcinogenesis. Aberrant activation of Wnt signaling causes β-catenin translocation to the nucleus and the regulation of gene expression that are involved in tumorgenesis such as MMPs, cyclin D1, and VEGF (*12*). Oncogenic mutation of K-*ras* results in activation of Ras and its downstream signaling pathways, such as the PI3K/Akt pathways (*13*). AKT activation leads to the inhibition of glycogen synthase kinase (GSK-3β), which fails to phosphorylate β-catenin, causing its accumulation in the cytoplasm and promotion of cell proliferation, angiogenesis, invasion, and metastasis.

It has been known that inflammation is causally linked to carcinogenesis and acts as a driving force in premalignant and malignant transformation (*14*). Previous studies have shown that inducible nitric oxide synthase (iNOS) and inducible-type cyclooxygenase (COX-2) could contribute to colon tumorigenesis by production of nitric oxide (NO) and prostaglandin E_2 (PGE_2) in AOM-induced rat and mouse colon cancers (*15*, *16*). Pterostilbene has been known to be an antioxidant and anti-inflammatory compound (*1*). In the present study, we examined the effect of pterostilbene on AOM-induced ACF formation and inflammatory activity and explored the underlying signaling molecular pathways. Our results show that pterostilbene significantly decreased ACF and adenoma formation of colon through induction of apoptosis and down-regulation of Wnt/β-catenin and EGFR/PI3K/Akt signaling pathways.

MATERIALS AND METHODS

Reagents. AOM was purchased from Sigma Chemical Co. (St. Louis, MO). Pterostilbene was synthesized according to the method reported by Pettit et al. (*17*). The purity of pterostilbene was determined by HPLC as >99.2%.

Animals. Male ICR mice at 5 weeks of age were purchased from the BioLASCO Experimental Animal Center (Taiwan Co., Ltd.). After 1 week of acclimation, animals were randomly distributed into control and experimental groups. All animals were housed in a controlled atmosphere (25 ± 1 °C at 50% relative humidity) and with a 12 h light/12 h dark cycle. Animals had free access to food and water at all times. Food cups were replenished with fresh diet everyday. All animal experimental protocols used in this study were approved by Institutional Animal Care and Use Committee of the National Kaohsiung Marine University (IACUC, NKMU) (*4*).

Identification of ACF and Adenomas. As described previously(*18*), a group of mice were given AOM at a dose of 5 mg/kg via an intraperitoneal (ip) injection of AOM twice a week for 2 weeks. Mice were given pterostilbene (50 or 250 ppm) supplement for 2 weeks along with AOM administration (**Figure 1**). The negative control group was injected with saline. At the end of week 6 or 23, the mice were sacrificed by decapitation and colons removed for evaluation of aberrant crypts or adenomas. The entire colons were excised, cut longitudinally, rinsed with ice-cold phosphate-buffered saline (PBS), and fixed flat between sheets of filter paper with 3.7% neutral formalin overnight. H&E stained sections were examined histologically and classified as ACF or adenomas according to specific pathological criteria established by a pathologist and referred to a previous paper (*19*). The formalin-fixed colonic tissues were cut into proximal (1−2 cm from the cecum), middle (3−4 cm), and distal (1−2 cm from anus) segments and stained in 0.2% methylene blue solution for 10 min. The total number of ACF and the number of aberrant crypts (ACs) in each focus were counted under a microscope (×40). ACF were classified with the following morphological characteristics; the enlarged and elevated crypts relative to normal mucosa and the increased pericryptal space and irregular lumen. The large, dark-stained, elevated lesions were counted using a light microscope (*20*). The ACF location (distance from anus) and size (number of aberrant crypts) were recorded. The crypt multiplicity of lesions was determined by transforming the diameter (mm) to crypt multiplicity. Diameters were scored with an eyepiece graticule. Lesion diameters of ≥1 mm were defined as adenomas by light microscopy (*21*−*23*).

Western Blot Analysis and Ras Activation Assay. For protein analyses, total scraped colon mucosa were homogenized on ice for 15 s with a Polytron tissue homogenizer and lysed in 0.5 mL of ice-cold lysis buffer (50 mM Tris-HCl, pH 7.4, 1 mM NaF, 150 mM NaCl, 1 mM EGTA, 1 mM phenylmethanesulfonyl fluoride, 1% NP-40, and 10 mg/mL leupeptin) on ice for 30 min, followed by centrifugation at 10000*g* for 30 min at 4 °C. The samples (50 μg of protein) were mixed with 5× sample buffer containing 0.3 M Tris-HCl (pH 6.8), 25% 2-mercaptoethanol, 12% sodium dodecyl sulfate (SDS), 25 mM EDTA, 20% glycerol, and 0.1% bromophenol blue. The mixtures were boiled at 100 °C for 5 min and were subjected to stacking gel and then resolved by 12% SDS−polyacrylamide minigels at a constant current of 20 mA. Subsequently, electrophoresis was carried out on SDS−polyacrylamide gels. For Western blot analysis, proteins on the gel were electrotransferred onto the 45 μm immobile membrane (PVDF; Millipore Corp., Bedford, MA) with transfer buffer composed of 25 mM Tris-HCl (pH 8.9), 192 mM glycine, and 20% methanol. The membranes were blocked with blocking solution (20 mM Tris-HCl, pH 7.4, 0.2% Tween 20, 1% bovine serum albumin, and 0.1% sodium azide). The membrane was further incubated overnight at 4 °C with respective specific antibodies, at appropriate dilution (1:1000) using blocking solution with the primary antibodies including iNOS, anti-Bcl-2, anti-Bcl-XL, anti-Bad, anti-Bax, anti-β-actin, anti-VEGF, and phospho-PI3K(Tyr508) polyclonal antibodies (Santa Cruz Biotechnology, Santa Cruz, CA); COX-2 monoclonal antibodies (BD Transduction Laboratories, Lexington, KY); anti-poly(ADP-ribose) polymerase (PARP; UBI, Lake Placid, NY), anti-Bid, anti-caspase-8, anti-caspase-3, anti-caspase-9, anti-Fas, and Fas-L (Transduction Laboratory), anti-DNA fragmentation factor (DFF)-45/inhibitor of caspase-activated DNase (ICAD) antibody (MBL, Naka-Ku, Nagoya, Japan), phospho-Akt (Ser473) and Akt polyclonal antibody (Upstate Biotechnology, Lake Placid, NY), and anti-pGSK3β, anti-cyclin D1, and anti-β-catenin (cell signaling). The membranes were subsequently probed with anti-mouse or anti-rabbit IgG antibody conjugated to horseradish peroxidase (Transduction Laboratories) and visualized using enhanced chemiluminescence (ECL, Amersham). The densities of the bands were quantitated with a computer densitometer (AlphaImagerTM 2200 System). All of the membranes were stripped and reprobed for β-actin (Sigma Chemical Co.) as loading control. To measure the level of activated Ras (Ras-GTP) in colon mucosa, 100 μg of cellular lysates was determined using a Ras activation assay kit (Upstate Biotechnology) following the recommendations of the manufacturer.

Table 1. Inhibitory Effects of Pterostilbene on AOM-Induced Colonic ACF Development in Male ICR Mice[a]

				no. of foci containing					
				proximal		middle		distal	
treatment[b]	total no. of ACF per mice	total no. of AC per mice	no. of AC per focus	<7 crypts	≥7 crypts	<7 crypts	≥7 crypts	<7 crypts	≥7 crypts
AOM	80.0 ± 5.7[b]	895.7 ± 51.6	12.3 ± 3.3	8.7 ± 2.1	9.0 ± 1.7	4.7 ± 2.5	18.7 ± 6.4	7.0 ± 2.1	24.3 ± 5.5
AOM + 50 ppm PS	46.0 ± 4.4[c]	457.8 ± 85.0[c]	9.9 ± 0.9[c]	7.0 ± 4.0	2.7 ± 1.2[c]	8.3 ± 4.2	14.0 ± 1.0	5.0 ± 3.0	9.0 ± 5.3[d]
AOM + 250 ppm PS	36.7 ± 7.7[c]	370.5 ± 49.3[c]	8.9 ± 0.0[c]	4.7 ± 3.2	3.3 ± 0.6[c]	6.3 ± 0.6	8.7 ± 4.2[c]	7.0 ± 2.8	9.0 ± 2.0[d]

[a] Animals were treated as described in **Figure 1**. Crypt multiplicity is defined as the number of aberrant crypts in each focus, categorized as either <7 (small ACF) or ≥7 (large ACF) aberrant crypts/focus. Data are mean ± SD values. [b] Mice were fed basal diet or diet containing pterostilbene starting 1 day before the first AOM treatment for 6 weeks. [c] $p < 0.05$ versus the AOM treatment. [d] $p < 0.001$ versus the AOM treatment.

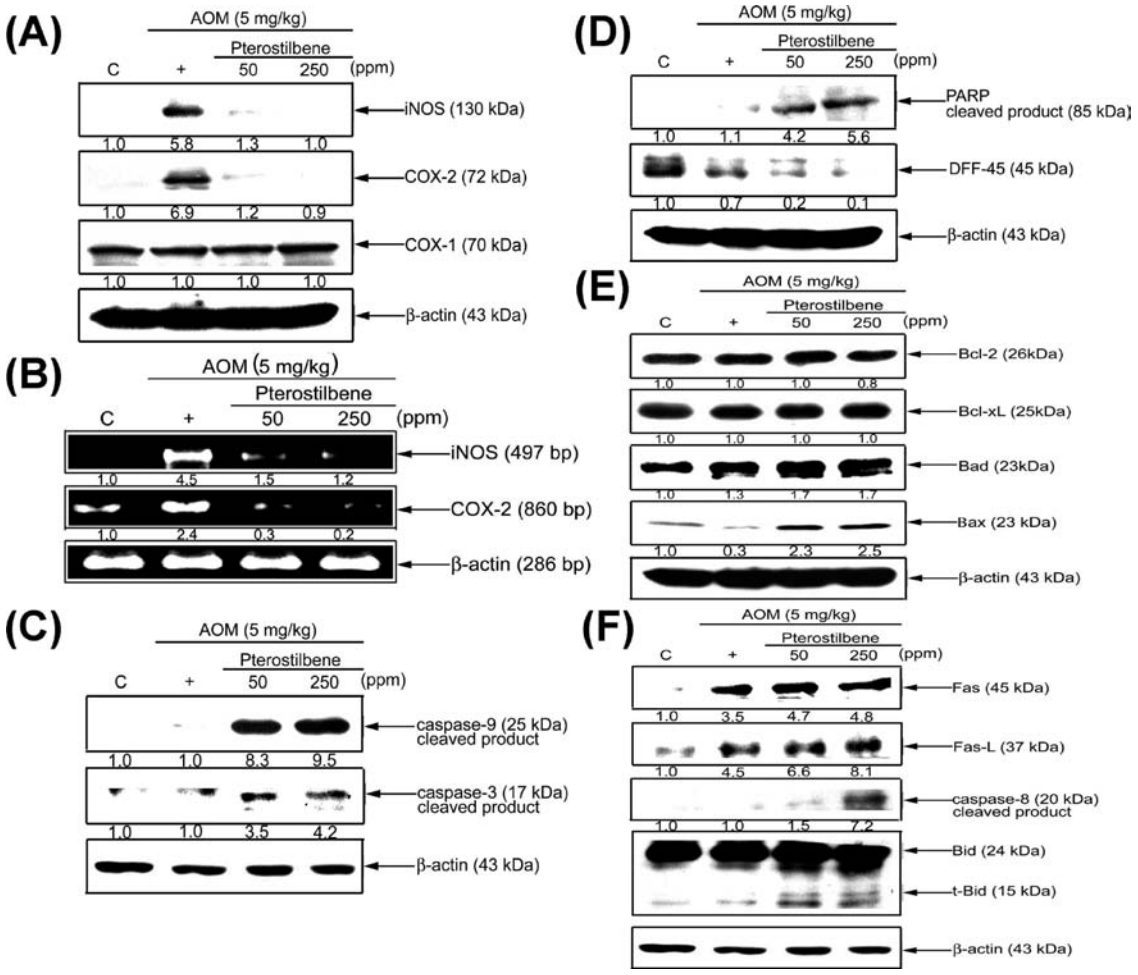

Figure 2. Effects of PS on AOM-induced inflammation- and apoptosis-related protein expression in male ICR mice. Male ICR mice were treated with pterostilbene (PS) at different concentrations, injected with AOM (5 mg/kg) or saline twice a week for 2 weeks, and then received basal diet alone or diet containing PS beginning 1 week after the last injection for 6 weeks. Normal and AOM-induced colonic mucosa from the indicated dietary groups were homogenized and lysates (50 μg of protein) subjected to Western blotting and RT-PCR as described under Materials and Methods. Pterostilbene inhibition of AOM induced iNOS and COX-2 protein (**A**) and gene expression (**B**). Dose-dependent cleavage of caspase-3, caspase-9, PARP, and DFF-45 was induced by pterostilbene (**C**) and (**D**). (**E**) PS affected expression of Bcl-2 family members in colon mucosa and AOM-induced ACF. Western blot analyses of Bcl-2, Bcl-xL, Bad, and Bax expression in normal crypt and ACF were performed as described under Materials and Methods. (**F**) Increase in the expression of Fas and Fas-L led to cleavage and activation of pro-caspase-8 and Bid during PS-induced apoptosis. The Western blot is representative of at least three independent experiments. Quantification of protein and gene expression was normalized to β-actin. The values under each lane indicate relative density of the band to β-actin.

Reverse Transcription−Polymerase Chain Reaction. Total RNA was extracted from scraped colonic mucosa using Trizol reagent according to the supplier's protocol. The template used was 4 μg of total cellular RNA in a 20 μL reaction solution with Super Script II RNase H-reverse transcriptase (Invitrogen, Renfrewshire, U.K.). The cDNA (2 mL) was amplified by Polymerase Chain Reaction (PCR) with the following primers: MMP-7 (493 bp) 5′-CAGATGTTGCAGAATACTCAC-3′ (sense), 5′-ATGCCTGCAATGTCGTCCT T T-3′ (antisense); cyclin D1 (409 bp) 5′- CTGACACCAATCTCCTCAACGAC-3′ (sense), 5′-GCGGCCAG-GTTCCACTTGAGC-3′ (antisense); β-actin (286 bp) 5′-AAGAGAGG-CATCCTCACCCT-3′ (sense), and 5′-TACATGGCTGGGGTGTTG-AA-3′ (antisense). PCR (GeneAmp PCR System 9700, Applied Biosystems, Carlsbad, CA) amplification was performed under the following conditions: 30 cycles at 94 °C for 1 min, 50 °C for 1 min, and 72 °C for

2 min, followed by a final incubation at 72 °C for 10 min. PCR products were analyzed by 1% agarose gel and visualized by ethidium bromide staining. Amplification of β-actin served as a control for sample loading and integrity.

Gelatin and Casein Zymography. Total scraped colonic mucosa was lysed in lysis buffer (50 mM Tris-HCl, pH 7.4, 1 mM NaF, 150 mM NaCl, 1 mM EGTA, 1 mM phenylmethanesulfonyl fluoride, 1% NP-40, and 10 mg/mL leupeptin) on ice for 30 min, followed by centrifugation at 10000*g* for 30 min at 4 °C. Protein concentration was measured according to the Bradford method (Bio-Rad). The unboiled samples (protein from colon mucosa) were separated by electrophoresis on 10 or 15% SDS-PAGE containing 0.1% gelatin or casein.

After electrophoresis, gels were soaked in 2.5% Triton X-100 in dH_2O (2 × 30 min) at room temperature and then incubated in substrate buffer (50 mM Tris-HCl, 5 mM $CaCl_2$, 0.02% NaN_3, 0.5 mM $ZnCl_2$, and 1% Triton X-100, pH 8.0) at 37 °C or 18 h. Bands corresponding to activity were visualized by negative staining using 0.3% Coomassie blue in 50% methanol and 10% acetic acid.

Immunohistochemical Analysis. Three micrometer sections of colonic mucosa in ACF and adenomas segments were deparaffinized, rehydrated, and treated with 0.3% hydrogen peroxide (H_2O_2) for 15 min to block endogenous peroxidase. Sections were pressure cooked for (4 × 7 min) in 10 mM citrate buffer, pH 6.0 (Immuno DNA retriever with citrate, BIO SB, Inc., Santa Barbara, CA), to unmask epitopes. Sections were incubated with primary antibodies to Bax and β-catenin (1:100 dilution in PBS) for 1 h. Immunoreactivity was incubated with biotin-labeled secondary antibody and streptavidin−biotin peroxidase for 30 min each. 3,3′-Diaminobenzidine tetrahydrochloride (0.05%, DAB) was used as the substrate, and a positive signal was detected as a brown color under a light microscope. The detailed procedures for stained tissue analysis method were reported previously (*24*). Cytoplasm and nuclear staining were recorded with β-catenin ectopic expression. For Bax, the criterion for positive expression showed cytoplasmic staining for the immunoreactive score (IRS) for the percentage of positive cells, and the staining intensity was multiplied.

Statistical Analysis. Relative expression values are given as mean ± SD for the indicated fold of expression in colon mucosa of mice. A one-way Student's *t* test was used to assess the statistical significance between the AOM and the pterostilbene plus AOM-treated groups. A *P* value of < 0.05 was considered to be statistically significant.

RESULTS

Dietary Pterostilbene Treatment Inhibited ACF Formation. The effects of dietary administration of pterostilbene on AOM-induced colon tumorigenesis were evaluated, and the results are summarized in **Table 1**. After 6 weeks of dietary treatment with pterostilbene, the animals were killed and the entire colons were harvested. Colonic ACF were identified and analyzed under a light microscope after methylene blue staining. ACF mostly occurred in the distal colon. **Table 1** summarizes the total number of ACF per mouse, the total number of AC per mouse, and the number of foci containing fewer than seven or seven or more AC. All mice developed ACF in the colon 6 weeks after AOM treatment. Compared with the positive control group, dietary pterostilbene treatment at levels of 50 and 250 ppm dose dependently decreased the total number of ACF per mouse by 42.5 and 54.1% ($P < 0.05$), respectively, and decreased the total number of AC per mouse by 48.8 and 58.6% ($P < 0.05$), respectively. We subsequently categorized ACF based on the number of AC in each focus. The results showed the pterostilbene treatments decreased the number of foci in seven or more AC compared with the positive control group, especially in the proximal and distal colon.

Pterostilbene Suppressed AOM-Induced Inflammation and Induced Apoptosis in Colon Carcinogenesis. Because the inhibition of inflammatory genes such as iNOS and COX-2 may contribute to the suppression of ACF formation in colon carcinogenesis, it is important to determine whether dietary pterostilbene may inhibit AOM-induced iNOS and COX-2 levels in the colon. As shown in

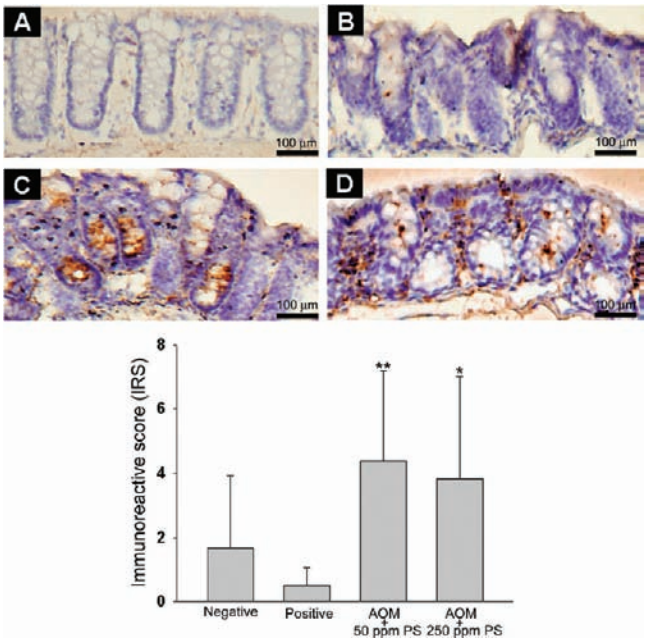

Figure 3. Immunohistochemical analysis shows increased Bax expression of colonic crypt in AOM-injected mice fed diet containing PS. At the end of week 6 (ACF group), the mice were sacrificed and determined by IHC methods. Staining (upper) and quantification (lower) patterns of Bax expression: normal mucosa of the negative control mice (**A**); ACF of the AOM treated positive mice (**B**); ACF of AOM + 50 ppm PS-treated mice (**C**); AOM + 250 ppm PS-treated mice (**D**) (100× magnification, IHC). Bax-expressing cells are stained brown. (Graph) Each bar represents the mean ± SD of the averages of 12 mice scored. Results were statistically analyzed with Student's *t* test (*, $p < 0.01$, and **, $p < 0.05$, compared with the AOM-induced value).

Figure 2A,**B**, the animals fed 50 and 250 ppm pterostilbene markedly decreased AOM-induced iNOS and COX-2 gene and protein expression. As shown in **Figure 2**, pterostilbene markedly inhibited the iNOS and COX-2 gene and protein expression in colonic mucosa compared with the AOM-alone group. The amount of constitutive COX-1 protein was not affected by AOM treatment. The pro-apoptotic response of dietary pterostilbene in the colonic tissue of AOM-injected mice was next investigated by Western blot analysis. As shown in **Figure 2C**,**D**, pterostilbene caused a strong apoptotic effect. Western blot analysis has shown that dietary pterostilbene dose-dependently induced the processing of caspases-9 and -3 and its downstream substrates, poly(ADP-ribose)-polymerase (PARP) and DNA fragmentation factor (DFF)-45 proteins, compared with control diet-fed AOM-injected mice. Moreover, the expression of Bcl-2, Bcl-xL, Bad, and Bax in pterostilbene-treated mice was investigated. As shown in **Figure 2E**, the dietary administration of pterostilbene caused marked increase of these proteins compared with the AOM-alone mice. To assess whether pterostilbene promoted apoptosis via receptor-mediated pathway, Fas, Fas L, caspase-8, and Bid were determined by Western blotting. The result showed that dietary administration of pterostilbene also increased the expression Fas, FasL, activated caspase-8, and truncated Bid compared with the AOM-alone group. The data suggested that the cleavage of Bid by activating caspase-8 may be one of the mechanisms that contributed to the activation of mitochondrial pathway during pterostilbene-induced apoptosis compared with the AOM alone mice.

Furthermore, representative photographs of the immunohistochemical staining of Bax-positive (**Figure 3**, shown at ×100

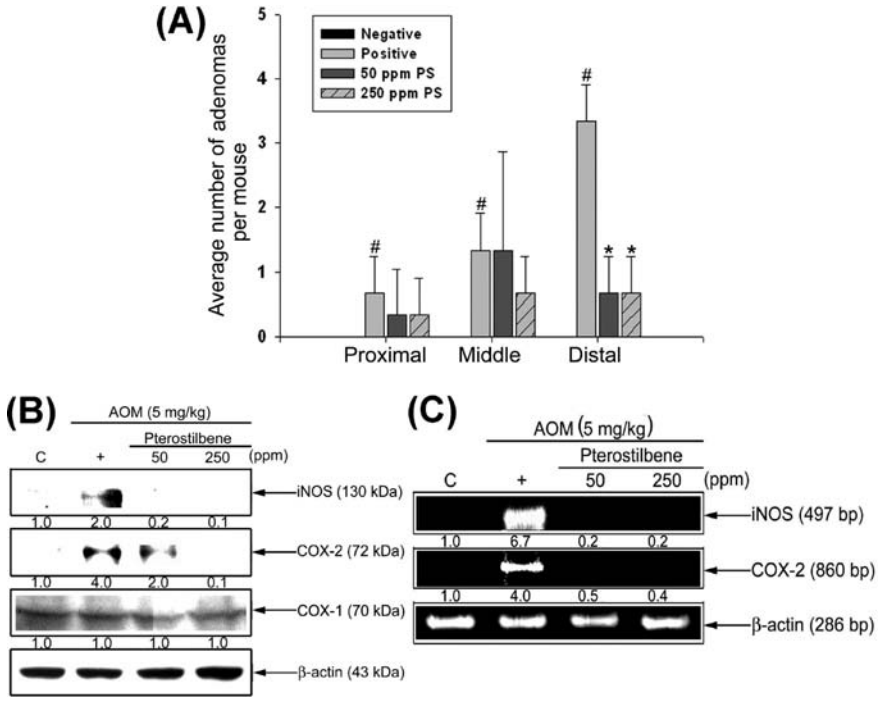

Figure 4. PS caused a statistically significant reduction of inflammation response in AOM-induced colon tumorigenesis. (**A**) Adenomas were fixed with 10% buffered formalin for 24 h and counted of adenoma number. The reduction of colon adenomas by PS was mainly due to inhibition in the number of rectal adenomas ($\geq$1 mm). AOM treatment induced a statistically significant ~5-fold increase in colon adenomas compared with saline-injected mice. Each bar represents the mean $\pm$ SD of the averages of 12 mice scored. Results were statistically analyzed with Student's *t* test ($*$, $p < 0.01$ compared with the AOM-induced value; #, $p < 0.001$ negative control (saline) vs AOM injected mice). Colonic mucosas from the indicated dietary groups were homogenized and lysates (50 μg of protein) subjected to Western blotting and RT-PCR as described under Materials and Methods. Pterostilbene inhibition of AOM induced iNOS and COX-2 protein (**B**) and gene expression (**C**). The Western blot is representative of at least three independent experiments. Quantification of protein and gene expression was normalized to β-actin. The values under each lane indicate relative density of the band to β-actin.

magnification) cells in AOM alone- and pterostilbene plus AOM-treated groups clearly show that pterostilbene increased the protein levels of Bax in colonic mucosa compared with the AOM-alone group.

Antitumor Activity of Pterostilbene in AOM-Injected Mice. The antitumor activity of dietary administration of pterostilbene on AOM-induced colon tumorigenesis was evaluated, and the results are shown in **Figure 4A**. The animals fed 50 and 250 ppm pterostilbene throughout 23 weeks were compared to the animals on the control diet. Pterostilbene treatment significantly reduced the number of adenomas in distal colon when compared with the AOM-alone group. Up-regulation of iNOS and COX-2 occurs in many pathological conditions, such as in tumorigenesis. From the results of this experiment, we have found that pterostilbene markedly reduced AOM-induced iNOS and COX-2 gene expression within the crypts in the adenoma in long-term feeding compared to those from the control group (**Figure 4B**,**4C**).

Pterostilbene Inhibits AOM-Induced Activation of β-Catenin by Inhibiting AOM-Induced Phosphorylation of GSK-3β. Colonic epithelial cell proliferation is under the control of the Wnt/APC/β-catenin proliferative signaling pathway (*25*). Inhibition of GSK-3β leads to an accumulation of β-catenin by decreasing the interaction of β-catenin with APC, which targets β-catenin for degradation. Aberration of β-catenin can be regarded as a key event during colorectal tumorigenesis and is linked to the increased transcription of a number of genes, such as cyclin D1, VEGF, and matrix metalloproteinases (MMPs) (*12*, *26*). The levels of phosphorylated GSK3β, β-catenin, VEGF, and cyclin D1 were markedly increased in colorectal tissues of AOM-treated mice compared to the control mice. Dietary administration of pterostilbene strongly decreased AOM-induced levels of these proteins (**Figure 5A**). We also found that AOM-treated animals showed decreased levels of E-cadherin as compared to the control animals. Pterostilbene treatment increased the levels of E-caderin. Accumulation of β-catenin causes Tcf-dependent transcriptional activation of growth-related genes to stimulate colon crypt proliferation. **Figure 6** shows the representative photographs of the immunohistochemical staining of β-catenin. β-Catenin was identified along the membrane of the epithelial cells in the negative control group (**Figure 6A**). The colonic crypt cells in the AOM-treated group showed homogeneous and intense staining for β-catenin in the cytosol and nucleus, with lower and scattered staining in the membrane. In contrast, the pterostilbene group had lower observable cytosol and nuclear staining compared with AOM-alone group (**Figure 6C**,**D**). Because cyclin D1, MMP7, and MMP-26 are downstream signaling targets of β-catenin, we determined whether pterostilbene reduced cyclin D1 and MMP-7 gene expression in colon adenomas. Pterostilbene treatment induced a decrease in the levels of AOM-increased cyclin D1 and MMP-7 mRNA, as evidenced by reverse transcription−PCR analysis (**Figure 5B**). In addition, pterostilbene dramatically blocked AOM-induced MMP-26 and MMP-7 enzyme activity (**Figure 5C**) and markedly inhibited the activation of MMP-2 and MMP-9 (**Figure 5D**), which was activated by MMP-7.

Inhibitory Effect of Dietary Pterostilbene on AOM-Induced Activation of Ras Signaling Pathway. Colon carcinogenesis is known to be a multistep process involving multiple genetic alterations. AOM-induced colorectal rodent adenomas exhibit *K-ras* mutations. Oncogenic mutations in Ras result in constitutive activation of Ras and its downstream signaling pathways,

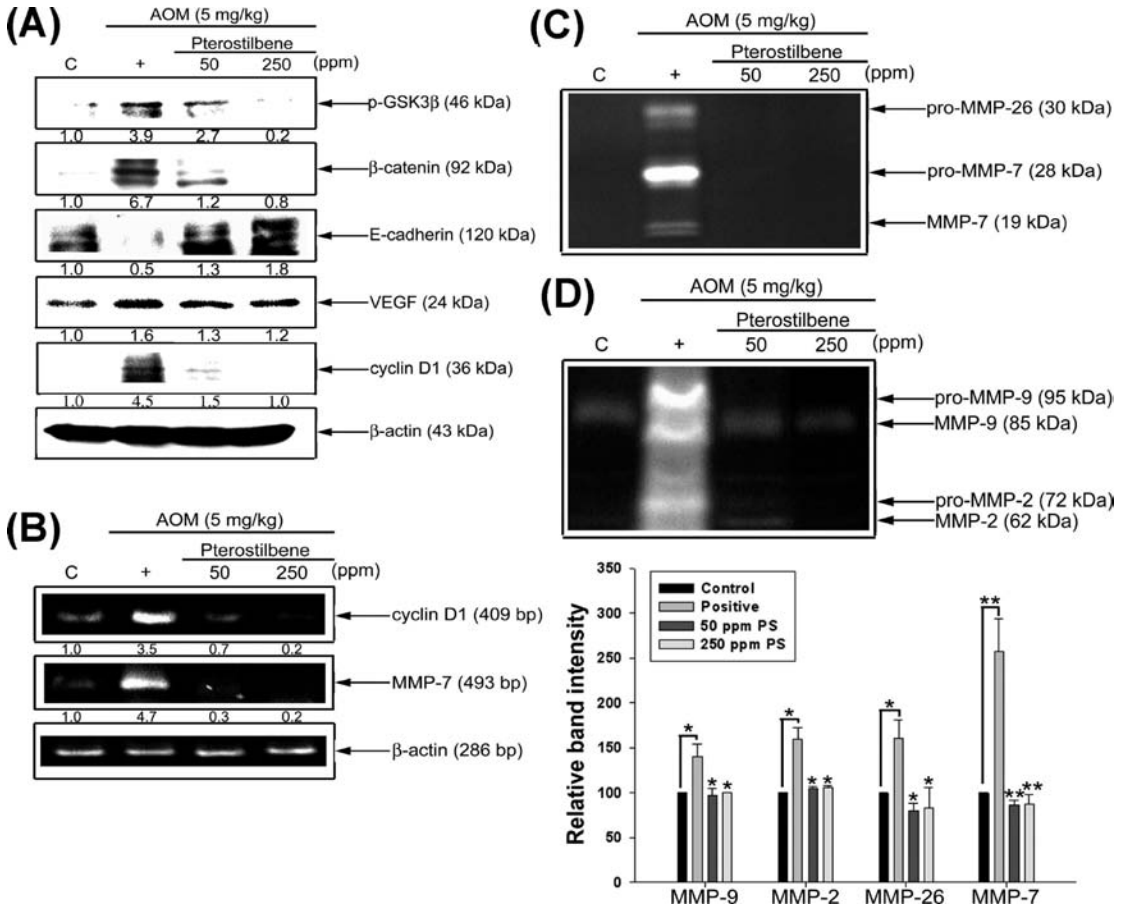

Figure 5. Effect of treatment with PS on AOM-induced Wnt/β-catenin signaling pathways in colonic mucosa. Male ICR mice were treated with pterostilbene (PS) at different concentrations and injected with AOM (5 mg/kg) or saline twice a week for 2 weeks and then received basal diet alone or diet containing PS beginning 1 week after the last injection for 23 weeks. (**A**) Equal amounts of cell lysates were subjected to Western blot analysis using antibodies against p-GSK3β, β-catenin, E-cadherin, VEGF, cyclin D1, and β-actin. (**B**) For RT-PCR analysis of β-catenin target gene, cyclin D1 and MMP7 primers were used. Each sample was normalized to β-actin. Cell lysates were subjected to 10% SDS-PAGE with 0.1% casein (**C**) and gelatin (**D**); the gelatinolytic activities of MMP-7, -26, -2, and -9 were determined by gelatin and casein zymography as described under Materials and Methods. The Western blot is representative of at least three independent experiments. Quantification of protein and gene expression was normalized to β-actin. The values under each lane indicate relative density of the band to β-actin. Results were statistically analyzed with Student's *t* test ($*$, $p < 0.05$, and $**$, $p < 0.001$, compared with the AOM-induced value). Each bar represents the mean $\pm$ SD of the averages of three independent experiments.

such as Raf/MEK/MAPK and PI3K/Akt/PKB pathways (*11*). AOM-treated animals showed increased levels of phosphorylated PI3K/Akt as compared to the control animals. Pterostilbene treatment markedly decreased AOM-induced increase in levels of PI3K/Akt in whole cell extract from colorectal tissues (**Figure 7A**). We also assessed whether Ras signaling was involved in AOM-induced tumorigenesis by performing kinase activity assay. Densitometric analysis of blots revealed significant increase Ras activity in colorectal tissues. We observed that dietary administration of pterostilbene attenuated AOM-induced activation of Ras. More importantly, no change was observed in the total mucosa Ras content compared with the AOM-treated group (**Figure 7B**). Additionally, as shown in **Figure 7C**, pterostilbene dramatically inhibited AOM-induced EGF and EGFR. Treatment of pterostilbene resulted in the inhibition of soluble EGF cleavage in mouse plasma as compared to that in the AOM-alone group (**Figure 7D**). The soluble EGF cleavages were associated with the activation of MMP-7 (*27*). The results suggest that increased ligand-induced activation of EGFR may be an important event for the development of the hyperproliferative state associated with induction of colorectal neoplasia. Dietary pterostilbene markedly abrogated AOM-induced multiple signaling including EGFR signaling pathways.

DISCUSSION

Chemoprevention is defined as the use of natural dietary compounds and/or synthetic substances to block, inhibit, reverse, or retard the process of carcinogenesis. Laboratory animal studies provide evidence that pterostilbene significantly suppressed AOM-induced formation of ACF and multiple clusters of aberrant crypts and inhibited AOM-induced iNOS expression (*6*). It is widely believed that misregulation of this pathway leads to the development of cancer. Reflecting this knowledge, the mechanism of action for many currently used anticancer agents is specifically targeted to regulate the apoptotic pathway, further stressing the role of programmed cell death in maintaining normal homeostasis. Research indicates that one of the mechanisms for some of these bioactives is through the signaling pathway inducing programmed cell death (*28*). Our recent study indicated that pterostilbene induced apoptosis in AGS cells through activating the caspase cascade via the mitochondrial and Fas/FasL pathway, GADD expression, and by modifying cell cycle progress and changes in several cycle-regulating proteins (*3*). COX-2 and iNOS are important enzymes involved in mediating the inflammation process, cell proliferation, and colon cancer (*15*). In the current study, we show that dietary administration of

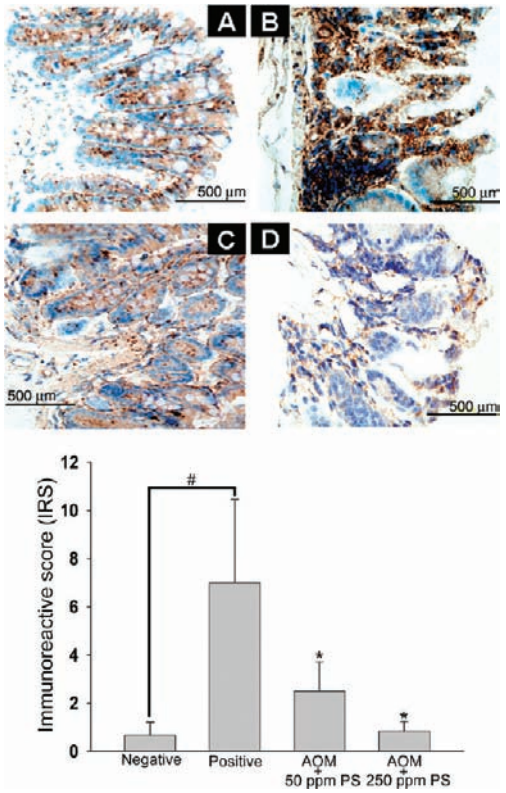

Figure 6. Cellular localization of β-catenin expression in AOM-treated mice. At the end of week 23, the mice were sacrificed and determined by IHC methods. Staining patterns of β-catenin expression: normal mucosa of the negative control mice (**A**); AOM treated positive mice (**B**); AOM + 50 ppm PS-treated mice (**C**); AOM + 250 ppm PS-treated mice (**D**) (400× magnification, IHC). (Graph) Each bar represents the mean ± SD of the averages of 12 mice scored. Results were statistically analyzed with Student's *t* test (∗, $p < 0.01$ compared with the AOM-induced value; #, $p < 0.001$ negative control (saline) vs AOM injected mice).

pterostilbene in two different protocols (6 and 23 weeks) dose-dependently inhibits the formation and development of AOM-induced colon tumorigenesis in mice. We clearly demonstrated that dietary administration of pterostilbene significantly inhibited AOM-induced iNOS and COX-2 and induced apoptosis in AOM-treated mice (**Figure 2**).

Increased cellular proliferation is a significant risk factor for the development of colon cancer (*11*). AOM reproducibly induces colon tumors that exhibit many of the same genetic and signal transduction defects identified in human colon carcinomas. AOM also induces ACF, which represent well-established preneoplastic colonic lesions in both animals and humans (*11*). Both the number and multiplicity of ACF are highly predictive of subsequent tumor development. Therefore, AOM-induced colon carcinogenesis is a highly relevant model for human colon cancer. Some studies have shown that a two-dose regimen in control rats induced colon tumors in 64% of animals; 53% had distal colon tumors, whereas only 30% showed proximal tumors (*29*). In the present study, we have demonstrated a positive correlation between the number of ACF and adenoma incidence. The distal region of colon had the highest number of ACF and adenomas followed by the proximal and middle colon (**Table 1** and **Figure 4**). Pterostilbene treatment significantly reduced the number of adenomas in distal colon, the segment previously also shown to have the greatest number of carcinogen-induced ACF and tumors (*30*). The greater ACF and adenoma frequency in the distal colon in this AOM mouse regimen may be explained by endogenous or exogenous factors. Recent evidence suggests that MMPs play a more complex role in tumor progression. They are necessary to create a microenvironment supporting the initiation and maintenance of growth of primary tumors and metastasis (*31*). Because epithelial−mesenchymal transition (EMT) and mesenchymal−epithelial transition (MET) are commonly associated with the acquisition of metastatic potential, we investigated whether pterostilbene suppressed AOM-induced EMT−MET. An important hallmark of EMT is the loss of membrane-bound E-cadherin in adherens junction. It is apparent that AOM induced EMT through inhibition of the levels of E-cadherin (**Figure 5A**), whereas pterostilbene treatment maintained the levels of E-cadherin. This is indicative of one of the molecular mechanisms through which β-catenin participates in EMT. Moreover, nuclear β-catenin localization strongly correlates with tumor size and dysplasia, and high levels of nuclear expression have been found at invasion fronts of adenocarcinomas (*32*).

Apoptosis and associated cellular events have a profound effect on the progression of a benign to a malignant phenotype and can be a target for the therapy of various malignancies including colon cancer (*28*). Thus, we examined the apoptosis-inducing effect of dietary administration of pterostilbene during AOM-induced ACF formation. Because caspase activation is one the most important events in apoptosis, and PARP and DFF-45 are major substrates of activated caspase-3, we also examined the levels of Fas and FasL by Western blotting to further confirm the apoptotic response of pterostilbene (**Figures 2** and **3**). The results of the present study clearly indicate that dietary pterostilbene induces apoptosis in a dose-dependent manner in the colon tissue of AOM-injected mice. Our results clearly show an in vivo apoptotic effect of pterostilbene that could, in part, be responsible for its overall efficacy in inhibiting AOM-induced ACF formation in mice colon. More studies are needed to define the underlying molecular events leading to in vivo apoptosis induced by pterostilbene in colorectal cancer models. Because pterostilbene at a low dose in the diet (0.005%) was shown to decrease the inflammation and increase apoptosis, the development of this natural compound against colorectal cancer could be promising.

On the basis of our finding, we suggest that pterostilbene promotes a strong protective effect against AOM-induced colon turmorigenesis by suppressing proliferation and enhancing apoptosis and down-regulation of early and long-term inside-out signaling processes. Our present study provides proof that, through a molecular mechanism, pterostilbene promotes a strong anticarcinogenesis effect via down-regulation of Wnt/β-catenin and EGFR/PI3K/Akt/PKB signaling pathways and then blocks NFκB and AP-1 transcription factors, as well as iNOS, COX-2, and MMPs. These promising results suggest the importance of further investigating pterostilbene in preclinical colon cancer models. Above all, our investigation suggests that pterostilbene has great potential as a novel chemopreventive agent to be used in the treatment of inflammation associated with tumorigenesis, especially in the prevention and treatment of colorectal cancer.

ABBREVIATIONS USED

AOM, azoxymethane; ACF, aberrant crypt foci; iNOS, inducible nitric oxide synthase; COX-2, cycoloxygenase-2; ICR, Institute of Cancer Research; VEGF, vascular endothelial growth factor; MMP-9, matrix metalloproteinase 9; PCR, Polymerase Chain Reaction; PI3K, phosphatidylinositol 3-kinase; PARP, poly(ADP-ribose) polymerase; EGFR epidermal growth factor receptor; GSK-3β, glycogen synthase kinase.

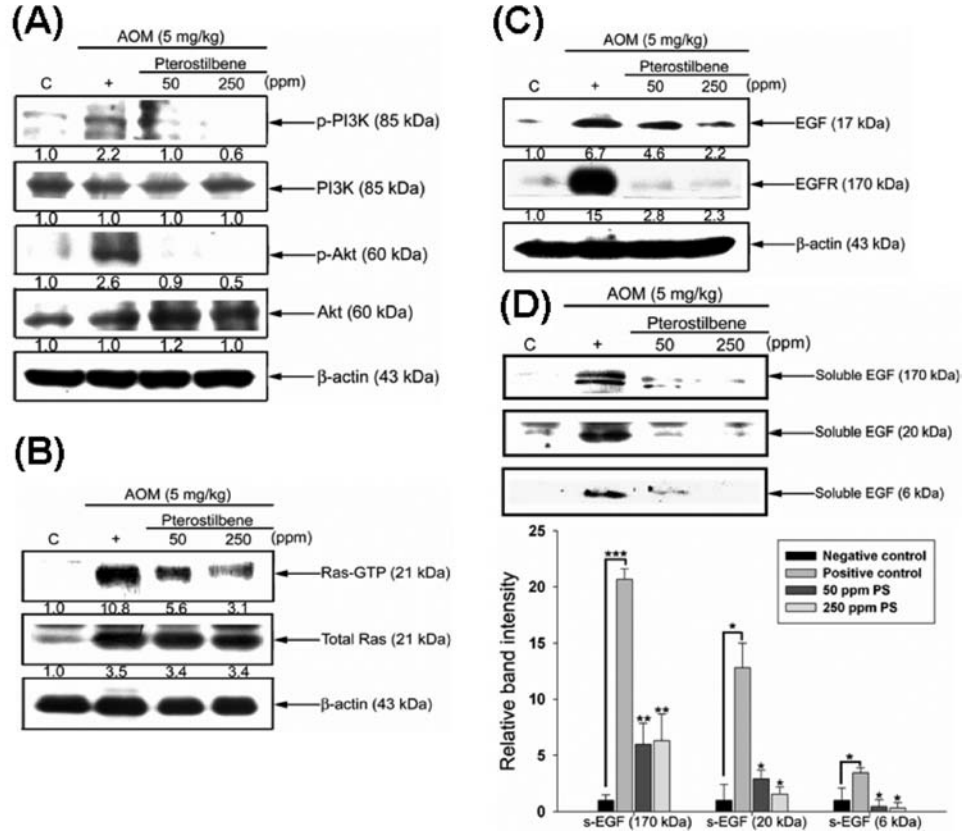

Figure 7. Modulation of crypt cell growth-regulatory proteins in the colonic mucosa of mice treated with AOM. Colonic mucosas from the indicated dietary groups were homogenized and lysates (50 μg of protein) subjected to Western blotting as described under Materials and Methods. (**A**) Western blot analysis of the levels of total and phosphorylated (p-) forms of PI3K and Akt in colon mucosa and AOM-induced adenomas. (**B**) Ras-GTP was affinity-purified with Raf-RBD-agarose and detected by anti-Ras immunoblotting. Total Ras levels from the same samples are shown below. (**C**) Dose-dependent inhibition of EGF and EGFR activated by pterostilbene. (**D**) Analysis of mouse soluble-EGF (s-EGF) containing molecules from plasma. The plasmas of s-EGF were assayed by Western blotting. (Graph) Each bar represents the mean ± SD of the averages of three independent experiments. The Western blot is representative of at least three independent experiments. Quantification of protein and gene expression was normalized to β-actin. The values under each lane indicate relative density of the band to β-actin.

LITERATURE CITED

(1) Remsberg, C. M.; Yanez, J. A.; Ohgami, Y.; Vega-Villa, K. R.; Rimando, A. M.; Davies, N. M. Pharmacometrics of pterostilbene: preclinical pharmacokinetics and metabolism, anticancer, antiinflammatory, antioxidant and analgesic activity. *Phytother. Res.* **2008**, *22*, 169–179.

(2) Pan, M. H.; Chang, Y. H.; Tsai, M. L.; Lai, C. S.; Ho, S. Y.; Badmaev, V.; Ho, C. T. Pterostilbene suppressed lipopolysaccharide-induced up-expression of iNOS and COX-2 in murine macrophages. *J. Agric. Food Chem.* **2008**, *56*, 7502–7509.

(3) Pan, M. H.; Chang, Y. H.; Badmaev, V.; Nagabhushanam, K.; Ho, C. T. Pterostilbene induces apoptosis and cell cycle arrest in human gastric carcinoma cells. *J. Agric. Food Chem.* **2007**, *55*, 7777–7785.

(4) Pan, M. H.; Chiou, Y. S.; Chen, W. J.; Wang, J. M.; Badmaev, V.; Ho, C. T. Pterostilbene inhibited tumor invasion via suppressing multiple signal transduction pathways in human hepatocellular carcinoma cells. *Carcinogenesis* **2009**, *30*, 1234–1242.

(5) Pan, M. H.; Lin, Y. T.; Lin, C. L.; Wei, C. S.; Ho, C. T.; Chen, W. J. Suppression of heregulin-β1/HER2-modulated invasive and aggressive phenotype of breast carcinoma by pterostilbene via inhibition of matrix metalloproteinase-9, p38 kinase cascade and Akt activation. *Evidence-Based Complement Alternat. Med.* **2009**, DOI: 10.1093/ecam/nep093.

(6) Suh, N.; Paul, S.; Hao, X.; Simi, B.; Xiao, H.; Rimando, A. M.; Reddy, B. S. Pterostilbene, an active constituent of blueberries, suppresses aberrant crypt foci formation in the azoxymethane-induced colon carcinogenesis model in rats. *Clin. Cancer Res.* **2007**, *13* (1), 350–355.

(7) Paul, S.; DeCastro, A. J.; Lee, H. J.; Smolarek., A. K.; So, J. Y.; Simi, B.; Wang, C. X.; Zhou, R.; Rimando, A. M.; Suh, N. Dietary intake of pterostilbene, a constituent of blueberries, inhibits the β-catenin/p65 downstream signaling pathway and colon carcinogenesis. *Carcinogenesis* **2010**, *31*, 1273–1278.

(8) Jemal, A.; Siegel, R.; Ward, E.; Hao, Y.; Xu, J.; Murray, T.; Thun, M. J. Cancer statistics, 2008. *CA Cancer J. Clin.* **2008**, *58*, 71–96.

(9) Fearon, E. R.; Vogelstein, B. A genetic model for colorectal tumorigenesis. *Cell* **1990**, *61*, 759–767.

(10) Volate, S. R.; Davenport, D. M.; Muga, S. J.; Wargovich, M. J. Modulation of aberrant crypt foci and apoptosis by dietary herbal supplements (quercetin, curcumin, silymarin, ginseng and rutin). *Carcinogenesis* **2005**, *26*, 1450–1456.

(11) Takahashi, M.; Wakabayashi, K. Gene mutations and altered gene expression in azoxymethane-induced colon carcinogenesis in rodents. *Cancer Sci.* **2004**, *95*, 475–480.

(12) Hlubek, F.; Spaderna, S.; Schmalhofer, O.; Jung, A.; Kirchner, T.; Brabletz, T. Wnt/FZD signaling and colorectal cancer morphogenesis. *Front. Biosci.* **2007**, *12*, 458–470.

(13) Kure, S.; Nosho, K.; Baba, Y.; Irahara, N.; Shima, K.; Ng, K.; Meyerhardt, J. A.; Giovannucci, E. L.; Fuchs, C. S.; Ogino, S. Vitamin D receptor expression is associated with PIK3CA and KRAS mutations in colorectal cancer. *Cancer Epidemiol. Biomarkers Prev.* **2009**, *18*, 2765–2772.

(14) Pan, M. H.; Lai, C. S.; Dushenkov, S.; Ho, C. T. Modulation of inflammatory genes by natural dietary bioactive compounds. *J. Agric. Food Chem.* **2009**, *57*, 4467–4477.

(15) Rao, C. V.; Indranie, C.; Simi, B.; Manning, P. T.; Connor, J. R.; Reddy, B. S. Chemopreventive properties of a selective inducible nitric oxide synthase inhibitor in colon carcinogenesis, administered

alone or in combination with celecoxib, a selective cyclooxygenase-2 inhibitor. *Cancer Res*. **2002**, *62*, 165–170.
(16) Takahashi, M.; Mutoh, M.; Kawamori, T.; Sugimura, T.; Wakabayashi, K. Altered expression of β-catenin, inducible nitric oxide synthase and cyclooxygenase-2 in azoxymethane-induced rat colon carcinogenesis. *Carcinogenesis* **2000**, *21*, 1319–1327.
(17) Pettit, G. R.; Grealish, M. P.; Jung, M. K.; Hamel, E.; Pettit, R. K.; Chapuis, J. C.; Schmidt, J. M. Antineoplastic agents. 465. Structural modification of resveratrol: sodium resverastatin phosphate. *J. Med. Chem*. **2002**, *45*, 2534–2542.
(18) Lin, S. Y.; Chan, H. Y.; Shen, F. H.; Chen, M. H.; Wang, Y. J.; Yu, C. K. Chitosan prevents the development of AOM-induced aberrant crypt foci in mice and suppressed the proliferation of AGS cells by inhibiting DNA synthesis. *J. Cell Biochem*. **2007**, *100*, 1573–1580.
(19) Ju, J.; Hao, X.; Lee, M. J.; Lambert, J. D.; Lu, G.; Xiao, H.; Newmark, H. L.; Yang, C. S. A γ-tocopherol-rich mixture of tocopherols inhibits colon inflammation and carcinogenesis in azoxymethane and dextran sulfate sodium-treated mice. *Cancer Prev. Res*. **2009**, *2*, 143–152.
(20) Bird, R. P.; Good, C. K. The significance of aberrant crypt foci in understanding the pathogenesis of colon cancer. *Toxicol. Lett*. **2000**, *112*−*113*, 395–402.
(21) Paulsen, J. E.; Loberg, E. M.; Olstorn, H. B.; Knutsen, H.; Steffensen, I. L.; Alexander, J. Flat dysplastic aberrant crypt foci are related to tumorigenesis in the colon of azoxymethane-treated rat. *Cancer Res*. **2005**, *65*, 121–129.
(22) Issa, A. Y.; Volate, S. R.; Muga, S. J.; Nitcheva, D.; Smith, T.; Wargovich, M. J. Green tea selectively targets initial stages of intestinal carcinogenesis in the AOM-ApcMin mouse model. *Carcinogenesis* **2007**, *28*, 1978–1984.
(23) Smith, D. L.; Keshavan, P.; Avissar, U.; Ahmed, K.; Zucker, S. D. Sodium taurocholate inhibits intestinal adenoma formation in APCMin/+ mice, potentially through activation of the farnesoid X receptor. *Carcinogenesis* **2010**, *31*, 1100–1109.
(24) Denkert, C.; Koch, I.; von, K. N.; Noske, A.; Niesporek, S.; Dietel, M.; Weichert, W. Expression of the ELAV-like protein HuR in human colon cancer: association with tumor stage and cyclooxygenase-2. *Mod. Pathol*. **2006**, *19*, 1261–1269.
(25) Pennisi, E. How a growth control path takes a wrong turn to cancer. *Science* **1998**, *281*, 1438–1441.
(26) Brabletz, T.; Jung, A.; Dag, S.; Hlubek, F.; Kirchner, T. β-Catenin regulates the expression of the matrix metalloproteinase-7 in human colorectal cancer. *Am. J. Pathol*. **1999**, *155*, 1033–1038.
(27) Ii, M.; Yamamoto, H.; Adachi, Y.; Maruyama, Y.; Shinomura, Y. Role of matrix metalloproteinase-7 (matrilysin) in human cancer invasion, apoptosis, growth, and angiogenesis. *Exp. Biol. Med*. (*Maywood*) **2006**, *231*, 20–27.
(28) Pan, M. H.; Ghai, G.; Ho, C. T. Food bioactives, apoptosis, and cancer. *Mol. Nutr. Food Res*. **2008**, *52*, 43–52.
(29) Holt, P. R.; Mokuolu, A. O.; Distler, P.; Liu, T.; Reddy, B. S. Regional distribution of carcinogen-induced colonic neoplasia in the rat. *Nutr. Cancer* **1996**, *25*, 129–135.
(30) Rao, C. V.; Hirose, Y.; Indranie, C.; Reddy, B. S. Modulation of experimental colon tumorigenesis by types and amounts of dietary fatty acids. *Cancer Res*. **2001**, *61*, 1927–1933.
(31) Chambers, A. F.; Matrisian, L. M. Changing views of the role of matrix metalloproteinases in metastasis. *J. Natl. Cancer Inst*. **1997**, *89*, 1260–1270.
(32) Brabletz, T.; Jung, A.; Hermann, K.; Gunther, K.; Hohenberger, W.; Kirchner, T. Nuclear overexpression of the oncoprotein β-catenin in colorectal cancer is localized predominantly at the invasion front. *Pathol. Res. Pract*. **1998**, *194*, 701–704.

Received for review April 25, 2010. Revised manuscript received July 8, 2010. Accepted July 8, 2010. This study was supported by the National Science Council (NSC 98-2313-B-022-002-MY3, 98-2321-B-022-001, and DOH098-TD-F-113-098007).